Chinese Journal of Chemistry, **2004**, *22*, 430—433 **Article**

Density Functional Theory and MP2 Calculations of the Transition States and Reaction Paths on Coupling Reaction of Methane through Plasma

YANG, En-Cui(杨恩翠) ZHAO, Xiao-Jun(赵小军) TIAN, Peng(田鹏)
HAO, Jin-Ku*(郝金库)

College of Chemistry & Life Science, Tianjin Normal University, Tianjin 300074, China

The two possible reaction paths of producing ethane on coupling reaction of methane through plasma were theoretically investigated by B3LYP and MP2 methods with 6-311G* respectively and further compared with the previous results calculated from B3LYP/6-31G*. The new investigated results consistently confirmed the previous conclusion. And the influences of the calculation methods and basis sets on the calculated results were also discussed.

Keywords density functional theory, MP2, transition state, reaction path, methane, plasma

Introduction

Recently, the natural gas has been gradually becoming one of the most potential resources of the world arising from its abundant content and little environmental pollution.[1] Therefore, lots of chemists have devoted themselves to developing and exploring novel chemicals with high additional values converted from methane. Indeed, the preparation of hydrocarbons from the coupling reactions of methane through plasma has attracted much attention both from theoretical chemists and chemical engineers and made rapid progress especially in recent years.[2] However, there are some inevitable difficulties encountered in practical experiments, such as low yield rate and selectivity. On the other hand, methane is always considered theoretically as one of the most stable molecules by organic chemists,[3] furthermore, it undoubtedly results in diversity and complexity of products due to the similarity of bond dissociation energy of C—H. Therefore, it is of great importance and necessity to investigate the reaction mechanism by theoretical methods. Thus, in this paper, we are interested to investigate the detailed reaction process theoretically, especially make a comparison with our previous results to examine the influences of calculation method and basis sets on the same system. We hope to afford some valuable results to the chemical engineers, theoretically.

Computational methodology

All *ab initio* molecular orbital (MO) calculations were performed by Gaussian98 package program[4] on a Pentium Pro IV computer.

The geometries involved in the reactions including reactants, transition states and products were fully optimized at the 6-311G* basis sets with density functional theory B3LYP[5] and unrestricted MP2[6] methods, respectively. The minimization was carried out using the Berny method[7] and the default parameters were used for the integral cut-off and minimization convergence criteria. TS command was employed to optimize all the structures of the transition states, which were further confirmed by harmonic vibration frequency analysis. To investigate the reaction minutiae, the minimum energy paths (MEP) were calculated by the intrinsic reaction coordinate (IRC) theory[8] at B3LYP/6-311G* with a gradient stepsize of 0.4 amu$^{1/2}$·bohr.

Result and discussion

In the previous paper,[9] we have suggested the possible reaction paths of producing ethane on the coupling reaction of methane through plasma based on the extensive literatures and our experiment facts, which were presented in Scheme 1. Herein, we would continue to report our systematically investigative results at 6-311G* basis sets with two different methods to offer a comparable result at the most.

Scheme 1 The possible elementary reactions on coupling reaction of methane to produce ethane

$$CH_4 + CH_2 : (\text{singlet}) \rightarrow C_2H_6 \quad (1)$$

$$CH_4 + CH_3\bullet \rightarrow C_2H_6 + H\bullet \quad (2)$$

* E-mail: encui@eyou.com
Received July 18, 2003; revised and accepted January 5, 2004.
Project supported by the Natural Science Foundation of Tianjin Education Commission (No. 20020902) and the Youth Fund Project of Tianjin Normal University (No. 52LE31).

The structures of the transition states

The structures of the transition state were optimized at B3LYP and MP2 methods with 6-311G* basis sets, respectively. The optimized geometrical parameters for TS by B3LYP are shown in Figure 1, and the main difference to TS optimized from MP2 method is listed in Table 1.

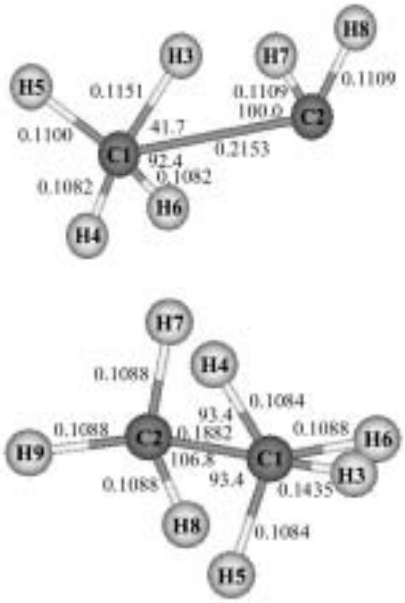

Figure 1 The structures of the transition states for the two paths optimized from B3LYP.

Table 1 The selected geometrical parameters and imaginary frequencies for the transition states calculated from MP2 and B3LYP (nm for bond length, (°) for bond angle and cm^{-1} for imaginary frequency)

Parameter	Path 1		Path 2	
	B3LYP	MP2	B3LYP	MP2
r_{C2C1}	0.2153	0.2238	r_{C2C1} 0.1882	0.1871
r_{H3C1}	0.1151	0.1128	r_{H3C1} 0.1435	0.1347
a_{H3C1C2}	41.7	40.1	a_{H3C1C2} 180.0	180.0
Imaginary frequency	−248.87	−234.69	−1419.86	−1875.95

The optimized transition states were further confirmed by vibration analysis, revealing that each of them had one and only one imaginary frequency as listed in Table 1. Compared with the two transition states optimized from the same method, the main difference consisted in the bond lengths of C1—C2, C1—H3 and the bond angle of H3C1C2. The bond length of C1—C2 of the TS in path 1 was longer than that in path 2, correspondingly, C1—H3 was shorter than that in path 2, indicating that the transition state of path 1 was nearer to reactants as compared with that of path 2. Interestingly at the TS location, the hydrogen atom H3, which would transfer to C2 in path 1, was in an angle of about 40° with C1 and C2, however, H3, which would leave from the system in path 2, was in alignment with C1 and C2. On the other hand, the geometrical parameters for the same TS located in two different methods have only shown an insignificant difference, which can be seen from Table 1. However, the very small difference in structure would lead to an appreciable influence on the total energy of the system.

The activation energy and the thermodynamic state functions of the two paths

To investigate the thermodynamic behavior of the two different reaction paths, the thermodynamic state functions including the standard formation enthalpy ($H^{o}_{m,f}$) as well as Gibbs free energy ($G^{o}_{m,f}$) and the sum energy of electrons including zero point correction energy for every species involved in the two paths were calculated and presented in Table 2. According to these data, the corresponding thermodynamic properties about the two reaction paths were further calculated and listed in Table 3.

Table 2 The relevant energy values of the species involved in the two paths (kJ/mol)

Species	E_T	$H^{o}_{m,f}$	$G^{o}_{m,f}$
MP2/6-311G*			
CH_4	−105817.18	−105807.18	−105868.79
CH_2:	−102318.61	−102308.68	−102365.01
CH_3•	−104113.36	−104102.68	−104165.42
Ini-C_2H_6	−208123.97	−208111.54	−208186.80
TS 1	−208121.86	−208108.38	−208185.33
TS 2	−209693.73	−209680.80	−209757.92
C_2H_6	−208595.51	−208583.97	−208656.13
H•	−1312.25	−1306.06	−1340.22
B3LYP/6-311G*			
CH_4	−106288.63	−106278.63	−106340.25
CH_2:	−102721.22	−102711.29	−102767.68
CH_3•	−104544.81	−104534.19	−104596.83
ini-C_2H_6	−209002.76	−208989.36	−209066.05
TS 1	−209001.23	−208988.36	−209063.80
TS 2	−210621.35	−210608.12	−210685.81
C_2H_6	−209445.67	−209434.06	−209506.36
H•	−1318.41	−1312.21	−1346.38
B3LYP/6-31G*[9]			
CH_4	−106262.50	−106254.98	−106252.50
CH_2:	−102687.87	−102677.94	−102736.08
CH_3•	−104517.61	−104507.15	−104569.63
ini-C_2H_6	−208948.77	−208931.98	−209016.60
TS 1	−208940.86	−208928.24	−209003.13
TS 2	−210556.48	−210554.00	−210631.63
C_2H_6	−209397.59	−209386.02	−209458.25
H•	−1313.47	−1306.23	−1347.26

Table 3 The activation energies and thermodynamic state functions of the two reaction paths [ΔE, $\Delta_r H_m^o$, $\Delta_r G_m^o$ in kJ/mol, $\Delta_r S_m^o$ in J/(mol· K)]

	Path 1			Path 2		
	MP2	B3LYP		MP2	B3LYP	
	6-311G*	6-311G*	6-31G*[9]	6-311G*	6-311G*	6-31G*[9]
ΔE	2.11	1.53	7.91	236.81	212.09	223.63
$\Delta_r H_m^o$	−468.11	−444.14	−453.10	19.83	66.55	69.88
$\Delta_r G_m^o$	−422.33	−398.43	−469.68	37.86	84.34	16.62
$\Delta_r S_m^o$	−153.55	−153.31	55.61	−60.47	−59.67	178.63

Note: $\Delta_r A = \sum A_{products} - \sum A_{reactants}$; $A = H_{m,f}^o$, $G_{m,f}^o$; $\Delta E = \sum E_{T\,TS} - \sum E_{T\,R(ini\text{-}complex)}$; $\Delta_r S_m^o = (\Delta_r H_m^o - \Delta_r G_m^o)/T$.

The data in Table 2 showed that the thermodynamic state functions and the total energy of the electrons for each species calculated from MP2 were consistently lower than those calculated from B3LYP. Furthermore, the total energy of the TS in path 2 was lower than that in path 1, which was reasonable because TS in path 2 had a hydrogen atom more than that in path 1 structurally. On the other hand, the data in Table 3 exhibited different characters of the two reactions both from thermodynamics and kinetics. Thermodynamically, path 1 was easier to occur than path 2 arising from more exothermic enthalpy and negative Gibbs free energy changes. Kinetically, the activation energy of path 1 is much lower than that of path 2, which undoubtedly decided that path 1 occurred easily. Therefore, we can conclude that path 1 is more favored than path 2 both from the viewpoints of thermodynamics and kinetics. Meanwhile, it was also easily observed that the activation energy and the thermodynamic function calculated from MP2 were uniformly higher than those from B3LYP and the sum energy of the electrons was decreased, but the activation energy and thermodynamic properties involved in the reactions were increased with the enlargement of the basis sets.

The intrinsic reaction coordinate (IRC) analyses

To investigate the reaction minutiae in more details, the intrinsic reaction coordinates of the two reaction paths were calculated at the same basis sets with B3LYP method. The potential curves were traced from TS by decreasing the energy with 0.4 amu$^{1/2}$·bohr, together with it we also obtained the structural variation during the whole reaction process, which were shown in Figures 2, 3 and 4, respectively.

Compared with the previous results, [9] it could be found that although the basis sets employed in the calculation were enlarged, they gave similar reaction process as shown in Figure 2, that is, isolated reactants→*ini*-complex (*ini*-C_2H_6)→TS→product for path 1 and reactants→TS→product for path 2. In addition, it can be seen that the location of the transition state in path 1 was obviously an early transition state as compared with that of path 2. The potential curve for path 1 indicated that once the reaction was solicited, it only demanded a very low energy barrier to form the transition state and then the total energy of the system gradually decreased

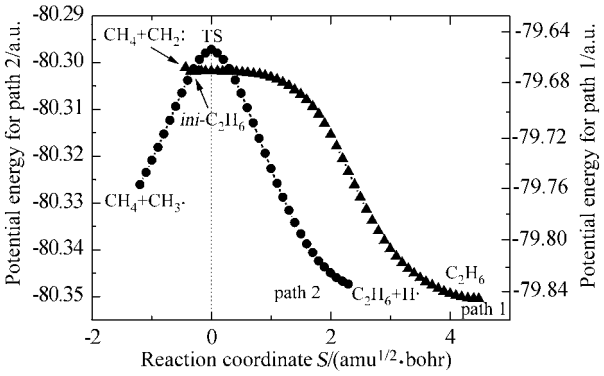

Figure 2 The potential energy curves along the reaction coordinate for the two paths.

and formed ethane slowly, which demanded a rather long process to finish. While in path 2, the system apparently needed to climb a relative high barrier to get to the transition state and form the products very soon. During the whole reaction process, the detailed variations of the system structure are shown in Figures 3 and 4.

Firstly, the structural parameters at both starting and ending points of IRC analysis in Figures 3 and 4 further validated that the transition state could connect the corresponding reactants and products, meaning that the two transition states located were indeed the transition states that belonged to paths 1 and 2, respectively. Secondly, the alteration of the systematic structure, whether the transfer or the leaving of hydrogen atom during the whole reaction process as shown in Figure 3 and 4, was synchronous and simultaneous and totally different from the photo-chlorinated process of pyridine.[10] Finally, the IRC analysis revealed that the geometry adjustment during reaction process mostly incarnated the reactive position, for example, only the bond lengths of C1—C2, C1—H3 and C2—H3 changed pronouncedly in both paths, while other bond lengths only varied a little, so we only gave the representative bond length alteration in Figures 3 and 4, which is similar to the bond angles.

Conclusion

The two possible paths about the coupling reaction of methane under plasma were investigated by B3LYP

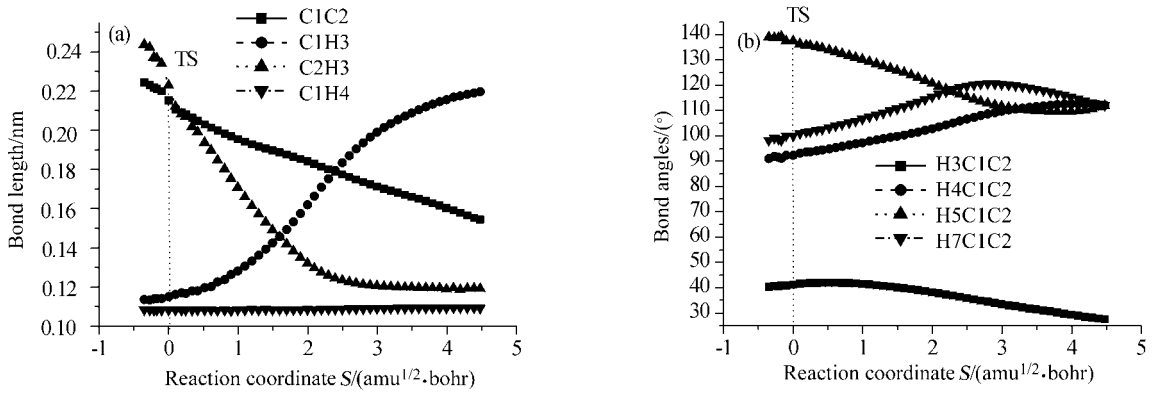

Figure 3 The structural variation along the reaction coordinate for path 1, (a) for bond lengths and (b) for bond angles.

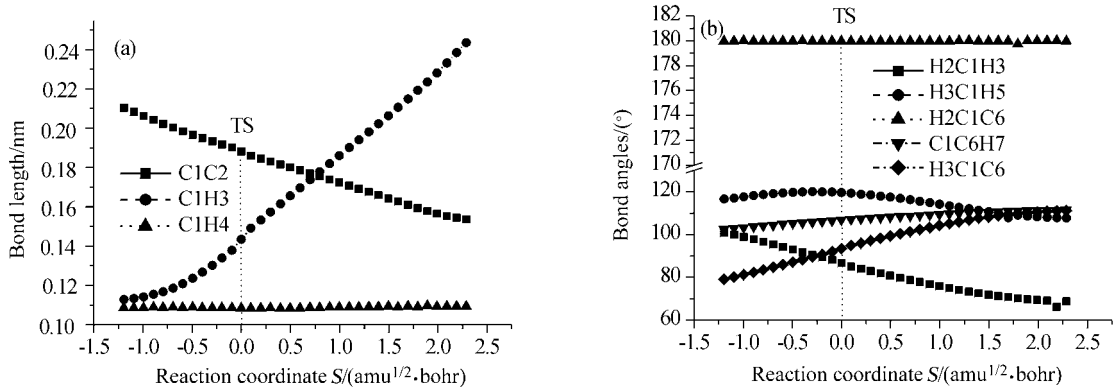

Figure 4 The structural variation along the reaction coordinate for path 2, (a) for bond lengths and (b) for bond angles.

and MP2 methods and 6-311G* basis sets. The calculated results revealed that compared with path 2, path 1 was much favored both from the viewpoints of kinetics and thermodynamics arising from relatively lower activation energy and more exothermic enthalpy as well as negative Gibbs free energy changes, which is in agreement with the previous calculated results.[9] In addition, the result also revealed that the energy for every species involved in the two paths calculated from MP2 method was uniformly lower than those from B3LYP method. While the activation energy and the thermodynamic state functions for the chemical reactions calculated by MP2 were consistently higher than those calculated by B3LYP method and the Gibbs free energy changes were greatly influenced by employing the enlarged basis sets as compared with the activation energy and enthalpy changes.

References

1 Campbell, C.-J. *Oil Gas J.* **1997**, *95*, 42.
2 Mohamed, B. *J. Catal.* **1996**, *161*, 282.
3 Guo, X.-M.; Chen, H.-F. *J. Chem. Engin.* **1995,** *46*, 304（in Chinese）.
4 Frisch, M. J.; Trucks, G. W.; Schlegel, H. B.; Scuseria, G. E.; Robb, M. A.; Cheeseman, J. R.; Zakrzewski, V. G.; Montgomery, J. A., Jr.; Stratmann, R. E.; Burant, J. C.; Dapprich, S.; Millam, J. M.; Daniels, A. D.; Kudin, K. N.; Strain, M. C.; Farkas, O.; Tomasi, J.; Barone, V.; Cossi, M.; Cammi, R.; Mennucci, B.; Pomelli, C.; Adamo, C.; Clifford, S.; Ochterski, J.; Petersson, G. A.; Ayala, P. Y.; Cui, Q.; Morokuma, K.; Malick, D. K.; Rabuck, A. D.; Raghavachari, K.; Foresman, J. B.; Cioslowski, J.; Ortiz, J. V.; Baboul, A. G.; Stefanov, B. B.; Liu, G.; Liashenko, A.; Piskorz, P.; Komaromi, I.; Gomperts, R.; Martin, R. L.; Fox, D. J.; Keith, T.; Al-Laham, M. A.; Peng, C. Y.; Nanayakkara, A.; Gonzalez, C.; Challacombe, M.; Gill, P. M. W.; Johnson, B.; Chen, W.; Wong, M. W.; Andres, J. L.; Gonzalez, C.; Head-Gordon, M.; Replogle, E. S.; Pople J. A. *Gaussian 98, Revision A.7*, Gaussian, Inc., Pittsburgh PA, **1998**.
5 Lee, C.; Yang, W.; Parr, R.G. *Phys. Rev. B* **1988,** *37*, 785.
6 Frisch, M. J.; Head-Gordon, M.; Pople, J. A. *Chem. Phys. Lett.* **1990**, *166*, 275.
7 Peng, C.; Ayala, P. Y.; Schlegel, H. B.; Frisch, M. J. *J. Compt. Chem.* **1996**, *17*, 49.
8 Fukui, K. *J. Phys. Chem.* **1970**, *74*, 4161.
9 Yang, E.-C.; Hao, J.-K.; Tang, T.-H.; Wang, B.-W.; Cao, Y.-Y. *Theochem* **2003**, *626*, 121.
10 Hao, J.-K.; Yang, E.-C.; Zhao, Z.-G.; Wang, G.-L.; Cao, Y.-Y.; Wang, Y.-X. *Acta Chim. Sinica* **2001,** *59*, 696 (in Chinese).

(E0307182 ZHAO, X. J.)